CHEMISTRY
A EUROPEAN JOURNAL

DOI: 10.1002/chem.200600002

A Triad Based on an Iridium(III) Bisterpyridine Complex Leading to a Charge-Separated State with a 120-μs Lifetime at Room Temperature

Lucia Flamigni,*[a] Etienne Baranoff,[b] Jean-Paul Collin,*[b] and Jean-Pierre Sauvage*[b]

Abstract: A triad **D**-**Ir**-**A**, where Ir is an Ir^{III} bisterpyridine complex connected through an amidophenyl spacer to D, a triphenylamine electron donor, and to A, a naphthalene bisimide electron acceptor, has been synthesized and electrochemically investigated. The photoinduced processes in the triad, which is more than 4-nm long, have been characterized by steady-state and time-resolved optical spectroscopy by comparison with the model dyads **D**-**Ir**, **Ir**-**A**, and the reference monomers **D**, **Ir**, and **A**. A sequential electron transfer occurs upon excitation of the D and Ir units, leading to the charge-separated state D^+-Ir^--A in 100% yield and subsequently to D^+-Ir-A^- in about 10% yield. The final charge-separated state has a lifetime at room temperature of 120 μs in air-free acetonitrile and of 100 μs in air-equilibrated solvent. Excitation of the A units does not yield intramolecular reactivity, but the resulting triplet-excited state localized on the acceptor, D-Ir-^{3}A, displays intermolecular reactivity.

Keywords: charge separation · electron transfer · iridium · photochemistry · supramolecular chemistry

Introduction

Charge separation is a key process for the conversion of light energy into chemical energy occurring in natural photosynthesis reaction centers. The most effective strategy for mimicking this process is based on multistep electron transfer triggered by light absorption in multipartite systems. A few impressive examples of long-lived charge-separated states in the millisecond range have been reported in the last decade in triads and upper homologues mainly based on tetrapyrrolic and/or fullerene units.[1] The use of arrays based on metal complexes has been rather limited and the results have been, in general, less satisfactory.[2] Only very recently a triad based on trisbipyridine–Ru^{II} and a $Mn_2^{II,II}$ complex was reported to exhibit a charge-separated state lifetime in the millisecond range at room temperature.[3] Long-lived charge-separated states have been reported also for simple dyads,[4] but some of the results are still the object of extensive debate in the chemical community.[5]

We have been active in the synthesis and characterization of covalently bound triads based on bisterpyridine metal complexes capable of displaying multistep electron transfer leading to charge separation over the extremities of the arrays. Several D-P-A triads, where D and A are electron donor and acceptor, respectively, and P is a Ru^{II}-, Os^{II}-, or Ir^{III}–bisterpyridine complex have been examined.[6] The use of terpyridine-type complexes as assembling units offers the advantage of producing linear arrays with the electroactive D and A units appended in opposite directions, without the problems of isomers arising from the use of bidentate ligands in an octahedral geometry. The serious limitation of low energy content and/or short lifetime of the excited state for Ru^{II} and Os^{II} derivatives was overcome by using Ir^{III}, the excited state of which has an high energy content (ca. 2.5 eV), and a remarkably long lifetime (1–2 μs or more).[7]

Following this strategy, we synthesized an Ir^{III}–bisterpyridine complex with a naphthalene bisimide electron acceptor (**A**) and a triphenylamine electron donor (**D**), and we report here the results obtained in the photogeneration of a remarkably long-lived charge-separated state in this triad. The array **D**-**Ir**-**A** (Scheme 1) is rigid and linear and well-suited for achieving charge separation over the terminal compo-

[a] Dr. L. Flamigni
Instituto ISOF-CNR
Via P. Gobetti 101, 40129 Bologna (Italy)
Fax: (+39) 051-639-9844
E-mail: flamigni@isof.cnr.it

[b] Dr. E. Baranoff, Dr. J.-P. Collin, Dr. J.-P. Sauvage
Laboratoire de Chimie Organo-Minérale
UMR 7513 CNRS, Université Louis Pasteur, Institut Le Bel 4, rue Blaise Pascal, 67070 Strasbourg (France)
Fax: (+33) 390-241-368
E-mail: jpcollin@chimie.u-strasbg.fr
sauvage@chimie.u-strasbg.fr

Supporting information for this article is available on the WWW under http://www.chemeurj.org/ or from the authors.

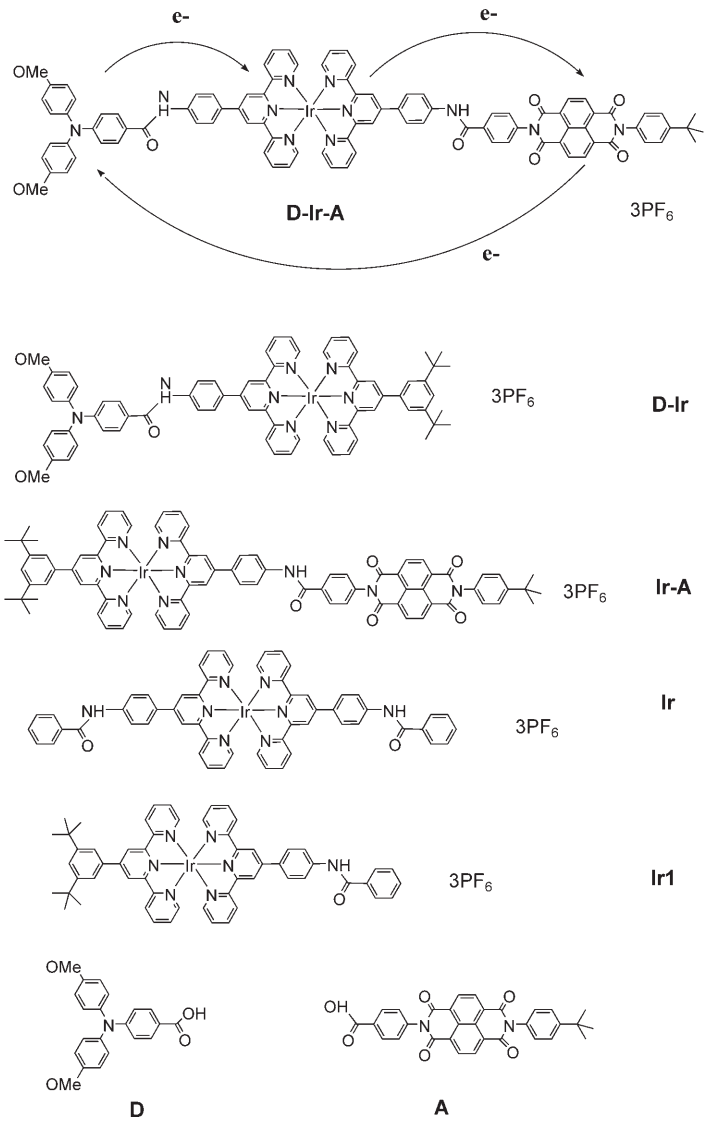

Scheme 1. Scheme showing structures of triad **D-Ir-A**, dyads **D-Ir** and **Ir-A**, reference monomers **D**, **Ir**, **A**, and reference compound **Ir-1**.

nents of the array (3.7 nm, D-to-A center-to-center distance). An iridium(III) bisterpyridine complex has a very high energy content in its excited state thus providing a high driving force for charge separation, furthermore the design of the system based on amide groups as linkers, which diminishes the electronic coupling between D and A, is expected to increase the lifetime of the charge-separated state. The selected A and D, an aromatic bisimide and an aromatic amine, respectively, are typical, widely used and well-characterized electroactive units for the construction of arrays able to undergo photoinduced charge separation.[8,9]

Results and Discussion

Design and synthesis strategy: A method combining a modular as well as a "chemistry-on-the-complex" approach has been used in relation to the chemical stability of the ligands in the usually harsh conditions required to substitute the iridium(III) coordination sphere. The reference compounds **A**, **Ir1**, and the dyad **Ir-A** have been prepared according to the reactions shown in Scheme 2.

The acceptor **A**, bearing a carboxylic function that is connected to the photoactive iridium(III) complex through an amide bridge, was synthesized in two steps from the commercially available 1,4,5,8-naphthalenetetracarboxylic dianhydride. In the first step, performed in dimethylacetamide as solvent, the use of an excess of the dianhydride leads to a moderate yield of the monosubstituted product (70%) because of its instability on the chromatographic support (SiO_2). The second imide formation, performed under more severe conditions (165°C) gave the acceptor **A** in 80% yield. Starting from the already described iridium complex **2**,[10] functionalized by an amine function, the reference compound **Ir1** and the dyad **Ir-A** were prepared in a straightforward manner by reaction with benzoyl chloride or **3**, in 64% and 46% yield respectively. In Scheme 3 the reactions leading to the triad **D-Ir-A** are reported. The terpyridine **6**, bearing a triarylamine donor group linked to the terpy fragment by an amide bridge, was prepared by condensation of **4** with **5** in the presence of *N*,*N*′-dimethylamino-4-pyridine (DMAP) and of *N*-(3-dimethylaminopropyl)-*N*′-ethylcarbodiimide hydrochloride (EDC) (peptidic coupling).[11,12] In the next step, the reaction of $IrCl_3$ with the terpyridine **6** in EtOH under reflux led to the intermediate **7** in low yield (30%), due to the poor solubility of ligand **6** in the reaction mixture. The experimental conditions of the coordination of the amino-terpyridine **5** with intermediate **7** are very critical since the amino group undergoes partial degradation in ethylene glycol under reflux. A short reaction time at 160°C is more favorable than prolonged heating. Purification of the crude material on TLC plates affords **8** in 42% yield. Eventually, the triad was obtained as an orange-yellow solid by reacting the precursor **8** with the acid chloride derivative **3**, leading to the triad **D-Ir-A** in 45% yield.

Electrochemistry: The redox characteristics of the reference compounds **Ir**, **Ir1**, **D**, **A**, the dyads **Ir-A**, **D-Ir**, and the triad **D-Ir-A** (see Scheme 1) examined by cyclic voltammetry in CH_3CN are reported in Table 1.

One-electron reversible waves were observed for all the redox processes. They were easily assigned to the corresponding individual components in each system. Due to the presence of amide bridges behaving as "insulators" between the various components of the dyads and of the triad, the redox potentials observed for the couples D^+/D, A/A^-, and terpy/terpy$^-$ are virtually independent of the structure of the compound that they belong to (dyads, triad, and reference compounds). Very weak interactions only are expected between the redox-active components in the dyads and in the triad. Therefore, a localized description of the individual subunits can be used with a high level of confidence to predict the exergonicity of energy and electron-transfer reactions.

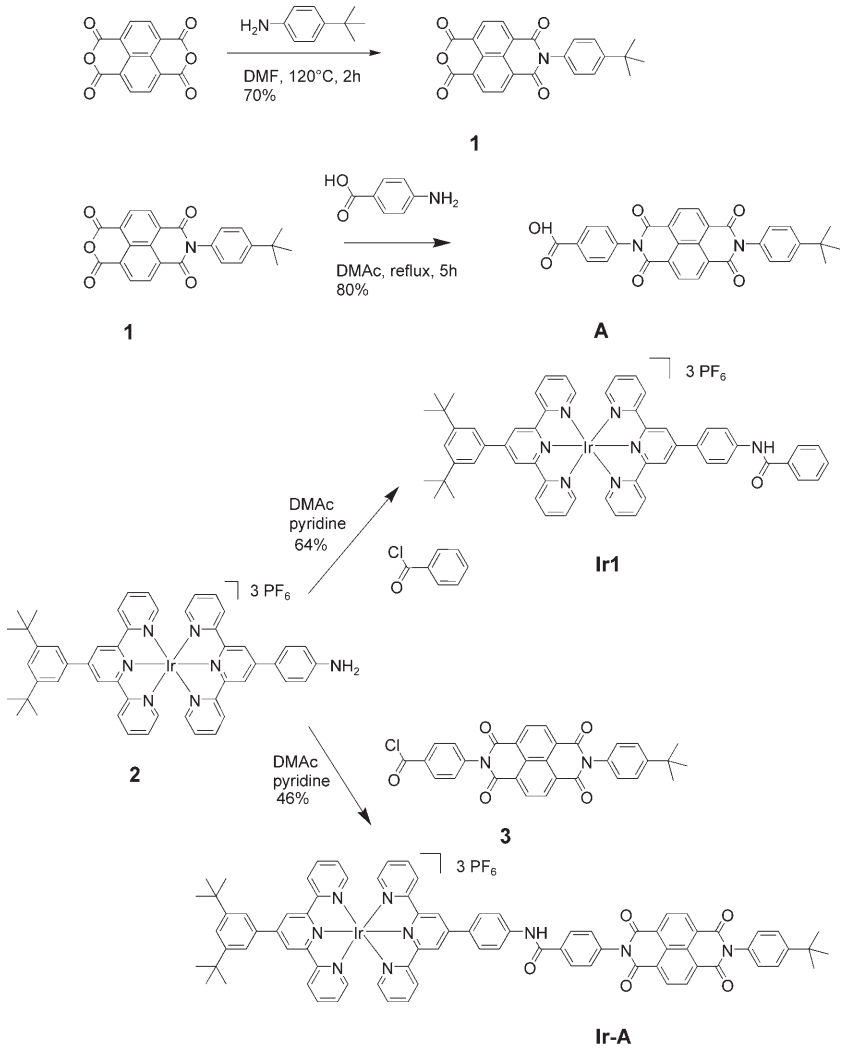

Scheme 2. Preparation of reference compounds **A**, **Ir1**, and dyad **Ir-A**.

Photophysical studies: The photophysical properties of the reference units **Ir1**, **Ir**, **D**, and **A**, the dyad components **Ir-A** and **D-Ir**, and the triad **D-Ir-A** depicted in Scheme 1 have been investigated. Characterization of **Ir1**, **D**, and **D-Ir** has been previously reported in a study on a series of dyads based on Ir^{III} bisterpyridine[10] and both **Ir1** and **Ir** have been the subject of a detailed study addressing the nature of the emitting excited state.[13] The results of previous investigations will be summarized briefly here to provide the reader with the necessary information to follow the overall discussion. It should be noted that whereas the complex **Ir1** is a good model for the metal complex in the dyads **D-Ir** and **Ir-A**, the best model for the complex in the triad **D-Ir-A** is the symmetric complex **Ir**.

Absorption spectroscopy: The absorption spectra in acetonitrile of the components, their superposition, and the experimental spectra of the arrays for the dyads **D-Ir**, **Ir-A**, and the triad **D-Ir-A** are shown in Figure 1. Whereas the experimental spectrum of dyad **Ir-A** displays a very good agreement with the absorption spectra calculated from the sum of the absorption coefficients of the models, the spectrum of the dyad **D-Ir** differs slightly from that calculated in that it shows a broadening of the absorption band on the low-energy side, up to 500 nm. A similar red shift and broadening compared to the calculated value, was also detected in the spectrum of the triad **D-Ir-A**. Moreover, some inconsistency between the calculated and experimental values can be observed in all spectra around 270–330 nm. Whereas the latter difference can be easily explained by the presence of one or two excess benzoic acid groups in the component models compared to the arrays (see Scheme 1), the red shift requires further comment. In $Ir(tpy)_2$-type complexes the low-energy absorption band is due, in general, to a predominantly ligand-centered (LC) transition leading eventually to a ^{3}LC emitting state characterized by high emission quantum yields ($\Phi_{em} \sim 0.02$) and long lifetimes ($\tau \sim 2$ μs) in air-equilibrated solutions.[14] Complexes of the $Ir(tpy)_2$-type with benzamide-appended terpyridine ligands were recently demonstrated to exhibit photophysical properties at room temperature ($\Phi_{em} \sim 0.002$ and $\tau < 1$ μs), typical of a charge-transfer (CT) state, either of metal-to-ligand charge-transfer nature (MLCT) or of intraligand charge-transfer nature (ILCT).[13] Addition of an aromatic system such as the triphenylamine **D**, which can further stabilize the CT excited state would shift the absorbance to lower energies. Williams and co-workers have recently reported a similar case, where substitution with an aliphatic amino unit in the terpy ligand leads to a red shift in the absorption spectra and to a scarcely emissive excited state. This was assigned to intraligand-charge-transfer transitions (ILCT), with the terpy ligand acting as an electron acceptor and the amine as an electron donor, responsible for an absorption band in the visible range.[15,16] However for the present purpose it is important to assess that interactions between components in the examined arrays are weak in order to use a localized description of the states involved in the photoinduced processes, and on the basis of the satisfactory

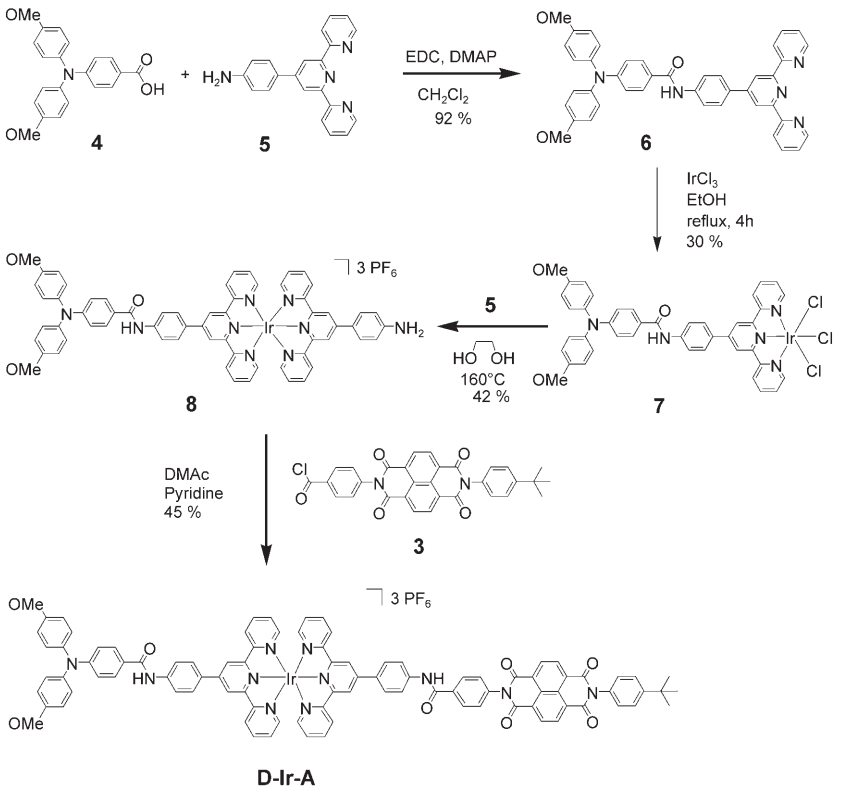

Scheme 3. Scheme to synthesis of triad **D-Ir-A.**

Table 1. Cyclic voltammetry data of the reference compounds **Ir**, **Ir1**, **D**, **A**, the dyads **D-Ir** and **Ir-A**, and the triad **D-Ir-A** in MeCN, 0.1 M nBu$_4$NPF$_6$, with SCE as reference.

	$E_{1/2}$/V (versus SCE)		
	D^+/D	A/A^-	terpy/terpy$^-$
Ir	–	–	−0.76
Ir1	–	–	−0.76
D	0.80	–	–
A	–	−0.54	–
D-Ir	0.75	–	−0.75
Ir-A	–	−0.44	−0.75
D-Ir-A	0.76	−0.50	−0.80

additive properties of the absorption spectra and of the electrochemical data we can safely assume a negligible electronic coupling between components.

Steady-state luminescence spectroscopy:

Room temperature: The luminescence spectra of the arrays **Ir-A**, **D-Ir**, and **D-Ir-A** in acetonitrile upon selective excitation of the Ir metal complex unit at 430 nm are shown in Figure 2 and compared to those of the models **Ir1** and **Ir**. A complete quenching of the excited state is detected in the dyad **D-Ir** and in the triad **D-Ir-A**, whereas only a partial quenching is detected for the metal complex luminescence in the dyad **Ir-A**. Though not selective (see Figure 1) the excitation of the A and D units in the arrays is also feasible and convenient wavelengths were found to be 320 nm to best excite the D unit, and 357 nm to excite the A unit with a favorable ratio, respectively.[17] The luminescence from the models at the two specified wavelengths were compared to those of the dyads and triad in conditions where the unit in the array absorbs the same number of photons as the pertinent model (see Figure 3). It should be noted that luminescence from **A** around 400 nm in acetonitrile is extremely weak ($\Phi_{em} \approx 2 \times 10^{-4}$) and it weakens on increasing the concentration above 10 μM because of the formation of excimers that display a broad emission band around 500 nm.[18] Excitation of the A unit in the dyad **Ir-A** and in the triad **D-Ir-A** results in the disappearance of the weak luminescence of A but it is difficult to assess if we are dealing with a genuine quenching. In fact, due to the spectral overlap of the emission with the absorption of **Ir-A** and **D-Ir-A** (see Figure 1), reabsorption of the weakly emitted light could be responsible for the lack of luminescence rather than a real quenching, as will be confirmed later by transient absorbance data. It should be noted that the emission of the Ir unit in the **Ir-A** array upon 357-nm excitation, calculated by taking into account the photons absorbed by the Ir unit alone (ca. 50 %), has the same yield as that obtained by its selective excitation at 430 nm (Table 2). This indicates that there is no sensitization of the triplet state localized on the complex, which would have been detected if quenching of the A unit were due to energy transfer from the Ir-^{1}A to ^{3}Ir-A state. As far as the D component is concerned, excitation of the D unit in both **D-Ir** and **D-Ir-A** arrays leads to a complete quenching of its strong luminescence (Figure 3).

77 K: From the luminescence experiments in butyronitrile glass of the models and arrays, the following qualitative conclusions can be derived: 1) A stronger quenching of the Ir unit than at room temperature is detected in **Ir-A** upon selective excitation at 430 nm, while the sensitized phosphorescence of the ^{3}A unit ($\lambda_{max} = 602$ nm) appears (see Figure S3 in the Supporting Information); 2) A slightly lower quenching of the Ir unit ($\lambda_{exc} = 410$ nm) than at room temperature occurs in **D-Ir** and **D-Ir-A** (see Figure S3 in the Supporting Information); 3) The D component appears similarly quenched in **D-Ir** and **D-Ir-A** as at room temperature on excitation at 320 nm; 4) The fluorescence of the A component

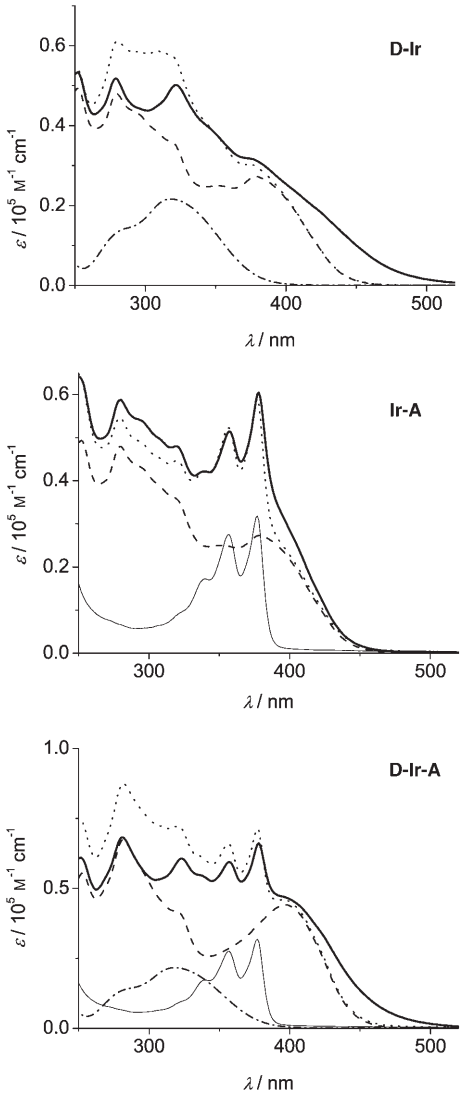

Figure 1. Absorption spectra of the model components and of the arrays. Upper panel: **Ir1** (– – –), **D** (–•–•), **D-Ir** (thick line), **Ir1**+**D** (•••••). Middle panel: **Ir1** (– – –), **A** (thin line), **Ir-A** (thick line), **Ir1**+**A** (•••••). Lower panel: **Ir** (– – –), **D** (–•–•), **A** (thin line), **D-Ir-A** (thick line), **D**+**Ir**+**A** (•••••).

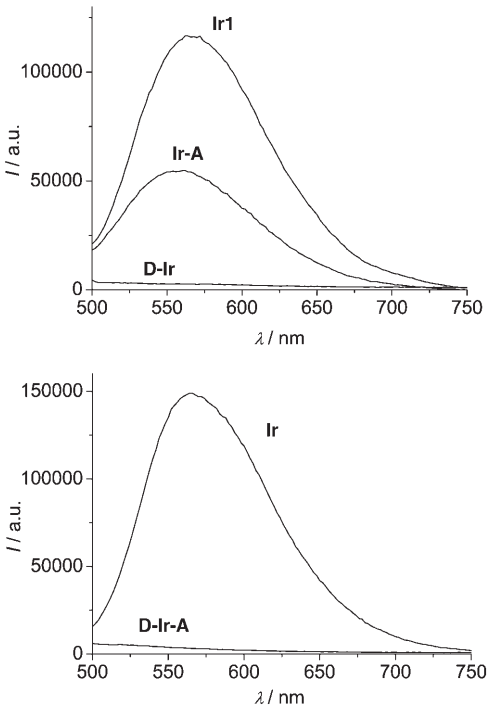

Figure 2. Luminescence spectra upon selective excitation of the iridium complex at 430 nm, $A = 0.2$, room temperature. Upper panel: Dyads **Ir-A**, **D-Ir**, compared to model **Ir1**. Lower panel: Triad **D-Ir-A** compared to model **Ir**.

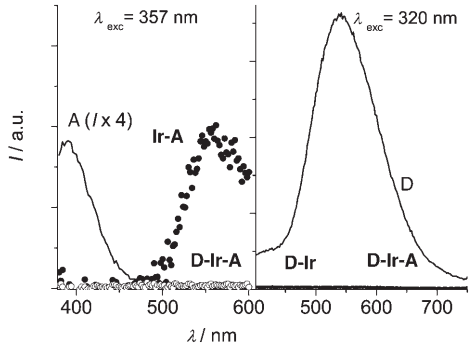

Figure 3. Room-temperature luminescence spectra of arrays and models in acetonitrile upon excitation at two selected wavelengths where the A and D components display high absorbances (see text). The absorbances of the solutions are arranged to provide the same number of photons absorbed by the model and the same unit in the arrays. In the right panel the signals from dyad **D-Ir** and triad **D-Ir-A** overlap.

($\lambda_{exc} = 357$ nm) is quenched similarly at 77 K and at room temperature in **Ir-A** and triad **D-Ir-A**, whereas the phosphorescence band due to the ^{3}A component, which can be detected in the model and in **Ir-A**, is absent in **D-Ir-A.** The emission data are summarized in Table 2.

Time-resolved luminescence spectroscopy: The luminescence lifetimes of the models **Ir1** and **Ir** in air-equilibrated acetonitrile solutions determined by using a single-photon nanosecond apparatus, were 490 ns and 580 ns, respectively.[13] The strong emission of the **D** model, presumably of CT character, was measured by a picosecond Streak Camera and had a lifetime of 450 ps.[10] The luminescence lifetime of the weak emission of the **A** model could not be detected in time-resolved experiments with a single-shot Streak Camera; the Raman scattering bands due to the solvent upon excitation at 355 nm obscured the useful spectral range 385–400 nm, and did not allow any reliable determination.

As far as the arrays are concerned, the Ir^{III} complex luminescence in **Ir-A** excited at 337 nm displayed a reduced lifetime with respect to the model **Ir**, 170 ns compared to 490 ns, in agreement with the steady-state luminescence data. Luminescence from the Ir component in **D-Ir** and **D-Ir-A** was not detected by a single-photon-counting apparatus

Table 2. Luminescence properties and energy levels of the excited states in air-equilibrated nitriles[a] of dyads **Ir-A**, **D-Ir,** and triad **D-Ir-A**, and models.

		295 K					77 K	
	State	λ_{max} [nm]	τ [ns]	Φ_{em}[b]	Φ_{em}[c]	Φ_{em}[d]	λ_{max} [nm]	E [eV][e]
Ir1	^{3}Ir	570	490	2.1×10^{-3}			510	2.43
Ir		566	580	2.7×10^{-3}			514	2.41
A	^{1}A	388	n.d.			$\approx2\times10^{-4}$	382	3.24
	^{3}A						602	2.06
D	^{1}D	540	0.450		0.012		422	2.93
Ir-A	^{3}Ir-A	562	170	1.0×10^{-3}		1.0×10^{-3}	510[f]	2.43
	Ir-^{1}A					$\leq6\times10^{-5}$		
	Ir-^{3}A						602	2.06
D-Ir	D-^{3}Ir			$\leq6\times10^{-5}$			515[g]	2.40
	D-^{1}Ir				$\leq6\times10^{-5}$			
D-Ir-A	D-^{3}Ir-A			$\leq6\times10^{-5}$			515[g]	2.40
	D-Ir-^{1}A					$\leq6\times10^{-5}$		
	D-Ir-^{3}A							
	^{1}D-Ir-A				$\leq6\times10^{-5}$			

[a] Acetonitrile at 298 K, butyronitrile at 77 K. [b] Luminescence quantum yields, excitation of Ir unit at 430. [c] Luminescence quantum yields, excitation at 320 nm.[17] [d] Luminescence quantum yields, excitation at 357 nm.[17] [e] Energy levels from the emission maxima at 77 K. [f] Excitation at 410 nm. [g] Weak signal.

with 0.5-ns resolution or by experiments with a single-shot Streak Camera with 20-ps resolution, and we detected no fluorescence signal around 540 nm upon excitation at 355 nm of the D component in **D-Ir** and **D-Ir-A**. This enabled us to assign a rate $k\geq5\times10^{10}\,s^{-1}$ to the quenching reaction of the Ir unit in **D-Ir-A** and of the D unit in **D-Ir** and **D-Ir-A**. The time-resolved luminescence data for the models and arrays are shown in Table 2.

Energy-level schemes: The processes can be conveniently discussed by making use of energy-level schemes that can be drawn from the luminescence data collected in Table 2 and from the electrochemical data reported in Table 1. The excited-state energies are derived from the maximum of the emission at 77 K (Table 2), whereas the charge-separated state energy levels can be calculated by adding the energy necessary to oxidize the potential donor and the energy necessary to reduce the potential acceptor in acetonitrile without further corrections. We will use the schematic energy level diagram in Figure 4 to describe the photoinduced processes introduced in the following sections.

Transient absorption spectroscopy: Since we are interested in the electron transfer occurring upon light irradiation expected to yield either the reduced or the oxidized radicals of the components, valuable information can be gained by transient-absorption techniques which, in addition to excited states, allow detection of all intermediates formed during the photoinduced reactions. The transient absorbance data for the dyads and triad solutions in air-equilibrated and air-free acetonitrile at excitation wavelength 355 nm are presented in Table 3. To help the characterization of the radicals produced by electron transfer, we performed a spectral characterization of the oxidized form of model **D**, D^+, and of the reduced form of model **A**, A^-, generated by chemical/photochemical methods (see Experimental Section for details). Figure 5 shows the resulting spectra and calculated molar absorption coefficients assuming a complete conversion of the starting material. The D^+ unit displays a peak at 760 nm and a minor broad band at 590 nm, whereas A^- is characterized by sharp peaks at 475 and 610 nm and broader peaks at 710 and 780 nm, in excellent agreement with previous reports.[19]

Notably, at the wavelength of laser excitation, 355 nm, all the components absorb light and this must be taken into account for the interpretation of the data for the dyads and triad. From Figure 1 the following partitioning of photons can be calculated: **Ir-A**: 50% on Ir and 50% on A; **Ir-D**: 70% on Ir, 30% on D; **D-Ir-A**: 10% on D, 45% on Ir, 45% on A.

Models Ir1, Ir, A, D: The transient-absorption spectra detected with picosecond resolution of optically matched solutions of the models in air-equilibrated solutions are shown in Figure 6. **Ir1** and **Ir** display a nearly identical strong absorption band, stable in the 3-ns window of the experiment, with a broad maximum around 780 nm. The **D** model gives rise to a sharp band at 750 nm with a lifetime of 490 ps, in agreement with the luminescence lifetime of 450 ps, indicating that the detected species is the singlet excited state ^{1}D. No residual absorbance ascribable to a triplet can be detected for **D** at 3.3 ns, the longest time probed by this experiment. The **A** model gives rise to an end-of-pulse spectrum with bands at 485 and 650 nm, and decays with a lifetime of 50 ps. The reported ^{1}A absorption spectrum and lifetime in toluene ($\lambda_{max}=510$ nm, $\tau=3$ ns)[20] are very different from our data. The differences could be justified by the influence of the polarity of the solvent that is known to have a strong effect on the photophysical parameters of bisimides[18] and the detected band could be assigned to the singlet excited state ^{1}A. Nonetheless, given the conditions of the experiments, performed with a concentration of the order of 30 μM, an excimeric nature of the band, that is, ^{1}AA, cannot be excluded.[21] The absorption decays to a much weaker maximum at 485 nm, which is stable over the time-window of the experiment (a few nanoseconds) and ascribable to the ^{3}A state (see below).

The components with a lifetime longer than a few nanoseconds can be conveniently probed by nanosecond laser flash photolysis. This allowed the derivation of lifetimes of 440 and 530 ns for the ^{3}Ir1 and ^{3}Ir states, respectively, in air-equilibrated acetonitrile solutions that are in good agreement with the luminescence lifetimes. In air-purged solutions the lifetimes increased to 740 ns and 1.75 μs, respectively, for the ^{3}Ir1 and ^{3}Ir states. No transient absorbance in

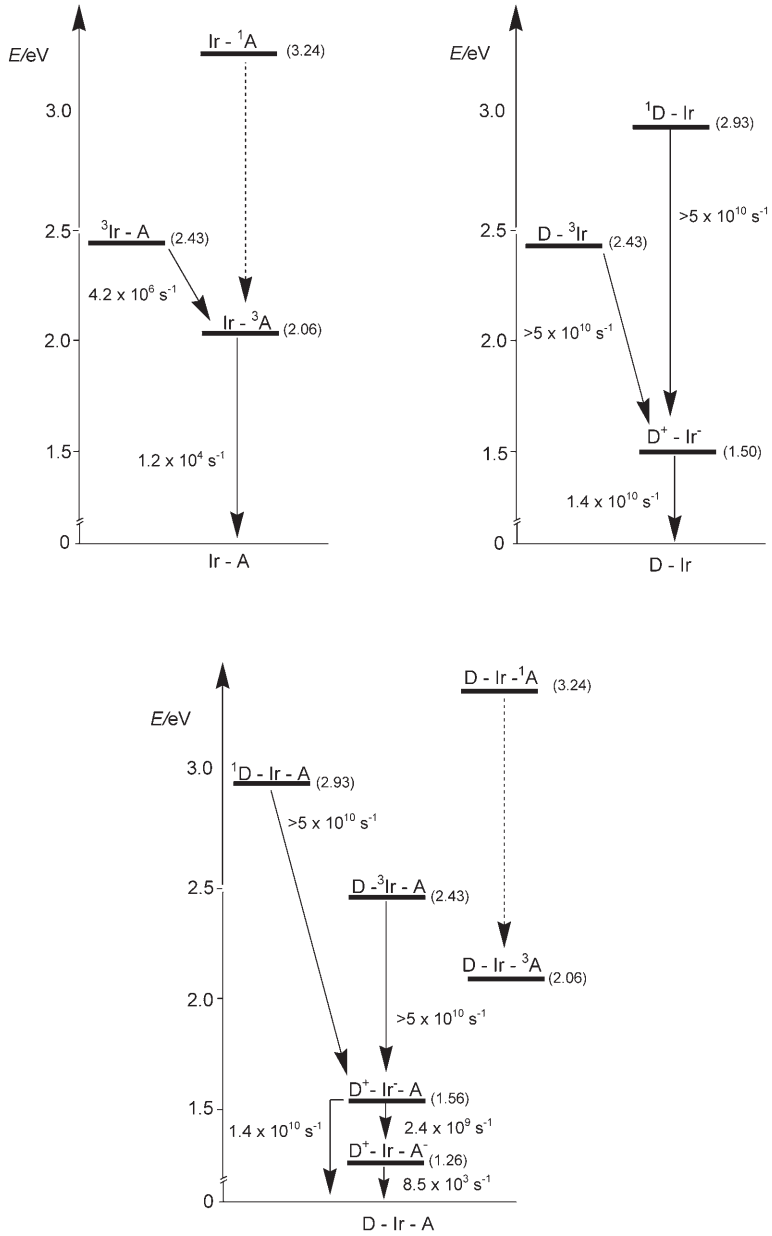

Figure 4. Energy level diagrams for dyads **Ir-A** and **D-Ir**, and triad **D-Ir-A**.

the nanosecond range can be recorded for solutions of model **D**, in agreement with the fast decay of the ^{1}D state and the lack of residual absorbance detected in the picosecond experiment. A solution of **A** displays upon laser excitation a band at 485 nm, which is assigned to the ^{3}A state in agreement with previous reports (Figure 7).[22] The triplet ^{3}A, formed with a quantum yield of approximately unity,[22] decays with a lifetime of 380 ns in air-equilibrated acetonitrile and 60 μs in air-free solutions, respectively.

Dyad Ir-A: In this dyad the end-of-pulse absorption spectrum detected in the picosecond experiment shows the intense and broad band assigned to the ^{3}Ir species at 780 nm and the peak assigned to the ^{1}A species at 485 nm, which undergoes intersystem crossing with a lifetime of 55 ps to the ^{3}A state (a similar lifetime was determined for the simple **A** model). This confirms that the singlet excited state of the acceptor unit does not undergo any intramolecular process and the intersystem crossing rate is not perturbed by the presence of the Ir complex. No further spectral change can be detected over the 3-ns window of the experiment. When a nanosecond laser flash photolysis experiment in oxygen-free solutions was carried out, a lifetime of 180 ns was measured for the decay of the band due to the ^{3}Ir-A species, shorter than that found in the model and in agreement with the 170-ns luminescence data. Upon its decay the typical band of ^{3}A at 485 nm was observed (Figure 8). The rise-time of the band due to the Ir-^{3}A species, $\tau = 180$ ns, was coincident with the decay of the ^{3}Ir-A species. The subsequent decay of the Ir-^{3}A species occurs with a lifetime of 60 μs, the same as that detected in the model ^{3}A state. The relative yields of formation of the triplet states ^{3}Ir-A and Ir-^{3}A can be calculated with respect to the models. By taking into account the photons absorbed by the unit of interest in the array at 355 nm, approximately 50% on each component, a yield of 1 is calculated for ^{3}Ir-A and a yield of about 2 is derived for Ir-^{3}A. These data confirm that there is a quantitative intramolecular energy transfer from the triplet ^{3}Ir-A to the triplet Ir-^{3}A state, whereas there is no sensitization of the triplet localized on the metal complex from an upper excited state. The reactions taking place in dyad **Ir-A** are summarized in Figure 4.

Dyad D-Ir: The photoinduced processes in this array have been reported recently.[10] In brief, electron transfer occurs from the excited state of both components with a rate faster than resolution (20 ps) to yield the charge-separated state D^+-Ir^- characterized by a band at 765 nm, with a broad shoulder between 570 nm and 700 nm, very similar to the spectrum of the oxidized donor D^+ determined by an inde-

Table 3. Transient-absorbance data in air-equilibrated or air-free[a] acetonitrile of dyads **Ir-A**, **D-Ir**, and triad **D-Ir-A**, and models following excitation at 355 nm.

		295 K		
	State	λ_{max} [nm]	τ [ns]	ϕ [b]
Ir1	^{3}Ir1	780	440 (740)	1
Ir	^{3}Ir	780	530 (1750)	1
A	^{1}A	485, 650	0.05	1
	^{3}A	485	380 (60×10^3)	1
D	^{1}D	750	0.490	1
Ir-A	Ir-^{1}A	485	0.055	
	^{3}Ir-A	745	(180)	1
	Ir-^{3}A	485	(180)[c] (60×10^3)	2
D-Ir[c]	^{1}D-Ir		$\leq$0.02	
	D-^{3}Ir		$\leq$0.02	
	D^+-Ir^-	765	0.070	1
D-Ir-A	D-^{3}Ir-A		$\leq$0.02	
	^{1}D-Ir-A		$\leq$0.02	
	D-Ir-^{3}A	485	360 (30×10^3)[d]	
	D^+-Ir^--A	765	0.06	1
	D^+-Ir-A^-	475, 610, 765	100×10^3 (120×10^3)	0.1

[a] Values for air-free solutions are in parentheses. [b] Relative yields of formation calculated on the basis of the photons absorbed by the unit of interest at 355 nm. [c] Lifetime of a rise. [d] The lifetime is concentration-dependent, see text; the reported value is at 1.8×10^{-5} M.

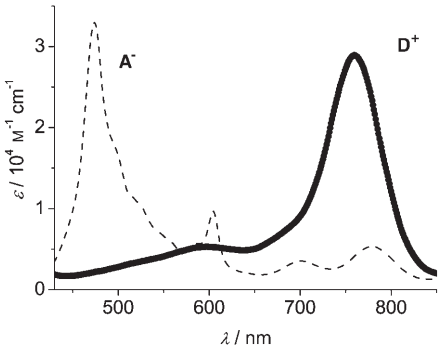

Figure 5. Absorption features of chemically generated A^- and D^+ species (see text for details).

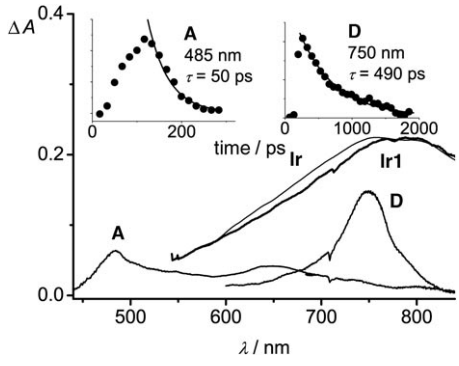

Figure 6. End-of-pulse absorption spectra of solutions of the models in acetonitrile upon excitation at 355 nm (4 mJ/pulse, 35 ps pulse). All solutions had $A=0.33$ at the excitation wavelength.

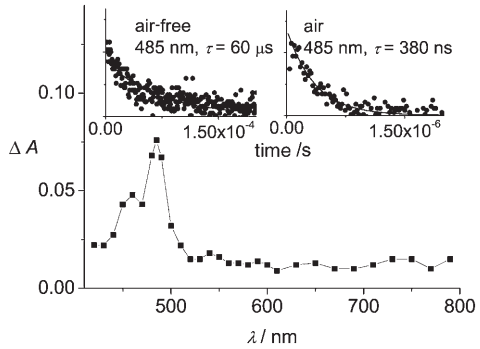

Figure 7. End-of-pulse absorption spectra of compound **A** solutions in acetonitrile ($A=1.3$), excitation at 355 nm (5.5 mJ/pulse, 18 ns pulse).

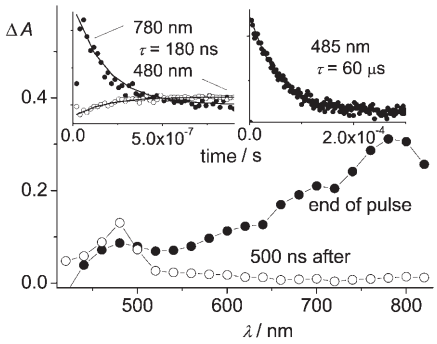

Figure 8. Absorption spectra of solutions of dyad **Ir-A** in air-free acetonitrile ($A=1.3$), excitation at 355 nm (5.5 mJ/pulse, 18 ns pulse).

pendent experiment. The decay of the charge-separated state (CS) takes place with a lifetime of 70 ps and no residual absorbance was detected for this array on the nanosecond timescale. The reaction taking place in dyad **D-Ir** and pertinent rates are summarized in Figure 4.

Triad D-Ir-A: The end-of-pulse spectrum detected with picosecond resolution in a solution containing triad **D-Ir-A** in acetonitrile upon excitation at 355 nm is shown in Figure 9. The spectrum shows a peak at 765 nm and two minor bands around 480 nm and 610 nm. The 765 nm band is typical of

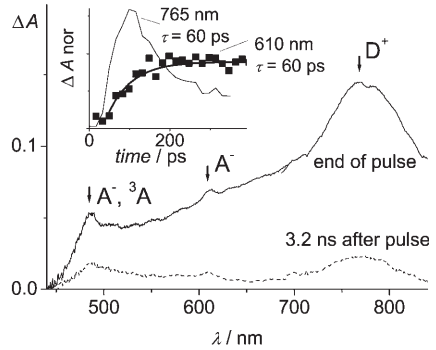

Figure 9. Transient-absorption spectra detected for a solution of triad **D-Ir-A** (1.6×10^{-5} M) in air-equilibrated acetonitrile after excitation at 355 nm (3.5 mJ/pulse, 35 ps pulse). The insets show the time evolution of the absorbance at 760 nm and a derived absorbance at 610 nm, reported on an arbitrary scale (see text).

the D^+ cation and (see above) can be assigned to the charge-separated states D^+-Ir$^-$-A and D^+-Ir-A$^-$, whereas the bands at 475 nm and 610 nm, typical of the A^- radical, are assigned to the charge-separated state D^+-Ir-A^-. The initial spectrum evolves, at the end of the experimental time window, into a spectrum still characterized by the same maxima, but with a different contribution of the A^- and D^+ components with respect to the initial one (Figure 9). The 475 nm band due to the A^- component overlaps with bands that have maxima around 485 nm assigned to the ^{3}A and ^{1}A (or ^{1}AA) components; for this reason the band at 610 nm is considered a better probe for the A^- radical. Since its contribution to the overall absorption at 610 nm is rather low but well-characterized as a sharp maximum on a rather flat background, we chose to measure the difference between the 610 nm absorbance and the background absorbance as a signature of the A^- anion. For this purpose we define, for each time delay, the transient differential absorbance $\Delta A(A^-) = \Delta A(610\text{ nm}) - [\Delta A(600\text{ nm}) + \Delta A(620\text{ nm})]/2$. A plot of $\Delta A(A^-)$ against time is shown in the inset of Figure 9, the time-evolution of which shows a fast rise with a lifetime of 60 ps, and is then stable over the following few nanoseconds probed by the experiments. On the other hand, the decay at 765 nm is fitted by a single exponential decay with a lifetime $\tau = 60$ ps,[23,24] in excellent agreement with the fast exponential rise detected at 610 nm, as shown in the inset of Figure 9, where the decay at 765 nm is reported in arbitrary units to allow a comparison with $\Delta A(A^-)$. These data indicate that the charge-separated state D^+-Ir$^-$-A ($\lambda_{max} = 765$ nm) decays to yield the fully charge-separated state (FCS) D^+-Ir-A^- ($\lambda_{max} = 610$ and 765 nm). Since the charge-separated state of the model dyad D^+-Ir$^-$ (see above) has a lifetime of recombination to the ground state $\tau_0 = 70$ ps, in the frame of the weak-interaction limit, we can assume that also D^+-Ir$^-$-A decays with the same rate to the ground state. This leads to a rate of formation of the fully charge-separated state $k_{FCS} = 1/\tau - 1/\tau_0 = 2.4 \times 10^9\ s^{-1}$ (Figure 4).

To follow the decay of the FCS state D^+-Ir-A^- that is stable over the approximately 3 ns time-window of the picosecond experiment, nanosecond laser flash photolysis experiments were performed. The end-of-pulse spectrum detected with nanosecond resolution in a flash photolysis experiment with an air-equilibrated solution of triad **D-Ir-A** is depicted in Figure 10 and is identical to that detected at 3 ns in the picosecond experiment, ascribable to the D^+-Ir-A^- charge-separated state. At early times a decay centered around 485 nm with a lifetime of 360 ns could be detected, see inset of Figure 10. This is identical to the decay lifetime of state ^{3}A (380 ns), and therefore assigned to the reaction of the triplet localized on the acceptor D-Ir-^{3}A with oxygen. The D-Ir-^{3}A species is formed by intersystem crossing of the D-Ir-^{1}A species directly formed by excitation of the array at 355 nm and does not display any specific intramolecular reactivity (see Figure 4). However, the bands assigned to the A^- and D^+ species are stable over several tens of microseconds. A decay is registered only on the hundreds of microseconds scale, Figure 10. The decay is rather complex, but a first-order decay with a 100 μs lifetime, independent from triad **D-Ir-A** concentration and laser energy, can be identified both on the band due to the anion (475 nm) and on the band due to the cation (760 nm). The residual spectrum still shows the presence of unreacted radicals and decays exponentially but with a relative weight and rate increasing both with triad **D-Ir-A** concentration and with the laser energy (Figure 11). The dependence of the decay rate on such parameters suggests a bimolecular nature for the slow decay whereas the 100 ± 10 μs component is independent of concentration of ground and excited species, typical of an intramolecular recombination. Therefore we assign the latter decay, essentially unaffected by solute concentration and laser intensity, to intramolecular charge recombination of the FCS state D^+-Ir-A^- to the ground state.

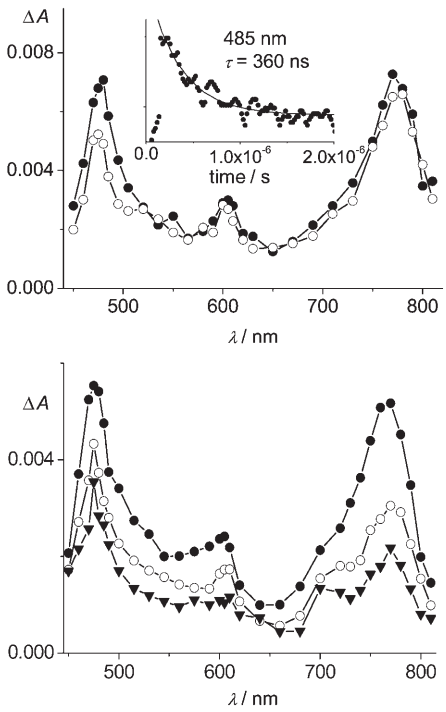

Figure 10. Transient-absorption spectra of solutions of triad **D-Ir-A** (1.8×10^{-5} M) in air-equilibrated acetonitrile upon excitation at 355 nm (1.9 mJ/pulse, 18 ns pulse). Top panel: End-of-pulse (●), 1.75 μs after the end of pulse (○). Bottom panel: 20 μs (●), 100 μs (○), and 200 μs (▼) after the pulse.

The slow and minor bimolecular component describing the decay of the radical bands can be explained as follows. Singlet oxygen ($^1\Delta_g$) is expected to be formed in the quenching reaction of the triplet D-Ir-^{3}A, as reported for the model **A**;[22] $^1\Delta_g$ is long-lived in acetonitrile, approximately 70 μs,[25] and could form a charge-transfer complex with the amine termini of a ground state triad **D-Ir-A**, eventually yielding a D^+-Ir-A species plus the superoxide ion O_2^-.[26] The superoxide ion O_2^- ($E_{1/2} = -0.78$ V for O_2/O_2^-[27]), could in turn transfer an electron to the A termini of a triad that is more easily reduced ($E_{1/2} = -0.50$ V), and lead to the formation of

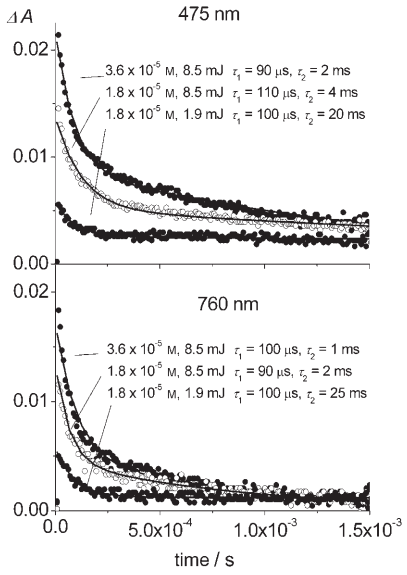

Figure 11. Decay of the bands assigned to the A^- (475 nm) and D^+ (760 nm) species in air-equilibrated acetonitrile and related fittings at different concentrations of triad **D-Ir-A** and laser energies; the 100 ± 10 μs decay is independent of concentration and laser energy.

the D-Ir-A^- species. Alternative routes for the formation of triad molecules bearing a single radical site could be the reaction of $^1\Delta_g$ or O_2 itself with the charge-separated state. In fact comparing the reactivity of the FCS state in air-free, see below, and air-equilibrated solutions, the charge-separated state appears to react slowly with O_2. Therefore a variety of secondary reactions originating from the triad (or its intermediate states) with oxygen in its ground and excited state can produce triad molecules with a single-radical site, either the D^+-Ir-A and/or D-Ir-A^- species. These are responsible for the minor, slow bimolecular decay of the bands due to radicals detected in air-saturated solutions. According to this mechanism, the importance of this contribution to the overall decay of the radical bands increases with the concentration and the photon flux, in perfect agreement with the experimental data.

Evaluation of the yield of the FCS state was performed by measuring the end-of-pulse band attributable to the A^- species against the actinometer benzophenone in benzene, and a value of the order of 7% with respect to the photons absorbed by the Ir and D units, was calculated (see experimental section for details).

When air is removed from the solution, the fast decay of the triplet D-Ir-^{3}A due to reaction with oxygen is not present, so that the spectrum does not show any change over the first few microseconds. The subsequent time evolution is shown in Figure 12 for a concentration of 1.8×10^{-5} M: A decay with a lifetime of 30 μs was measured at 485 nm for the triplet, shorter than that of the model ^{3}A, and a corresponding increase was found at 760 and about 605 nm for the bands of the cation and anion radical, respectively. The rate of decay of the triplet D-Ir-^{3}A at 485 nm and the formation of the radicals was found to depend on the concentration of triad **D-Ir-A** (Figure 13). In air-free solution, the long-lived triplet D-Ir-^{3}A can react with the ground state according to the reaction: D-Ir-^{3}A + D-Ir-A → D^+-Ir-A + D-Ir-A^- and yield donor and acceptor radicals localized on different triad molecules. In conditions of low concentrations of D-Ir-^{3}A, that is, at low laser energy, the experimental pseudo-first-order rate constant determined for the reaction k_{exp} is proportional to the solute concentration, [**D-Ir-A**], and can be expressed as $k_{exp}=k$[**D-Ir-A**]. The determined rate constants (k_{exp}) at the different concentrations are shown in the inset of Figure 13 with the linear plot that yields a bimolecular rate constant $k=2\times10^9$ M^{-1} s^{-1}. This is lower than the diffusion limit of 1.9×10^{10} M^{-1} s^{-1}, as expected from a diffusion reaction with a strict directional requirement; in fact the side of the triad containing the excited ^{3}A component has to come into contact with an other triad molecule at the D side.

As the triplet D-Ir-^{3}A is able to produce a reduced acceptor radical and an oxidized donor radical localized on different triad units by a reaction with a ground state, the subsequent decay of the radical bands will be due both to

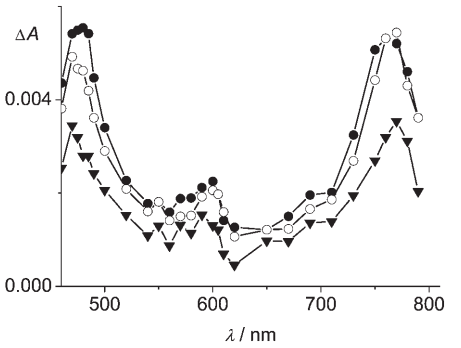

Figure 12. Transient-absorption spectra of solutions of **D-Ir-A** (1.8×10^{-5} M) in air-free acetonitrile upon excitation at 355 nm (1.9 mJ/pulse, 18 ns pulse), end-of-pulse (●), 50 μs (○), and 200 μs (▼) after the pulse.

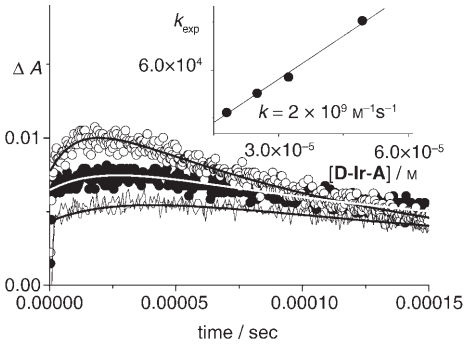

Figure 13. Time evolution of the 760 nm absorbance at different concentrations of triad **D-Ir-A** in air-free acetonitrile following excitation at 355 nm (1.5 mJ, 18 ns pulse): 2.5×10^{-5} M (line), 3.2×10^{-5} M (●), 4.9×10^{-5} M (○). In the inset the pseudo-first-order rate is reported versus concentration to derive the second-order rate constant.

an intramolecular recombination in the D^+-Ir-A^- species and to an intermolecular recombination of the radicals D^+-Ir-A and D-Ir-A^-. We could detect a strict first-order decay with a lifetime of about 120 μs, both at 475 nm, corresponding to the band of the reduced-acceptor, and at 760 nm, corresponding to the band of the oxidized donor (Figure 14).

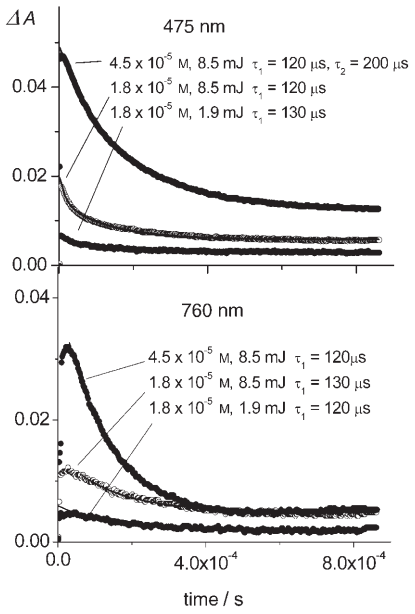

Figure 14. Decay of the bands assigned to the A^- (475 nm) and D^+ (760 nm) species in air-free acetonitrile and related fittings at different concentrations of triad **D-Ir-A** and laser energies; the 120 ± 10 μs decay is independent of concentration and laser energy.

This lifetime, like the one of 100 μs detected in air-equilibrated solutions is unperturbed by laser energy and ground-state concentration and therefore assigned to the intramolecular decay of the charge-separated state.[28] Also in this case, after the simple first-order decay of 120 μs, a residual spectrum is left, still containing the fingerprints of the donor cation and the acceptor anion. This slow decay occurs with a rather complex kinetics, strongly dependent on the laser energy and solute concentration; at extremely high laser energy and solute concentration it becomes faster and merges with the intramolecular decay (see Figure 13), whereas at a low laser energy and solute concentration the decay is exponential and has a lifetime of about 0.7 s. This type of behavior is expected for a bimolecular reaction.

Any further determination of homogeneous kinetics details is beyond our aim. For our purposes it is sufficient to assign the slow decay both in air-free and in air-equilibrated solutions to intermolecular reactions occurring in triad species having a single-radical site. These, either the D^+-Ir-A and/or the D-Ir-A^- species are formed upon diffusive reaction of the excited triplet D-Ir-^{3}A with oxygen (in air-equilibrated solutions) or with the ground state (in air-free solutions), and decay either by recombination or with some minor contaminant of the solution, depending on the experimental conditions. It is important to establish the existence of a strict mono-exponential decay ascribable to intramolecular recombination of the charge-separated state under a wide variety of experimental conditions.

Intramolecular photoinduced processes

Dyad Ir-A: Both components of this dyad are strong oxidants in their excited states. $E_{1/2} = -0.75$ V for the terpy-localized reduction of the Ir complex whereas the oxidation of complex **Ir1** was never determined within the usual potential ranges and it was assumed to occur at potentials higher than 2 V.[14] Reduction of the A unit occurs at $E_{1/2} = -0.44$ V, whereas oxidation can be expected above 2.5 V. Therefore on thermodynamic grounds electron transfer is very difficult from the excited state Ir-^{1}A and impossible from the excited state ^{3}Ir-A. Excitation of the acceptor in the dyad leads to the high-energy Ir-^{1}A excited state that decays unperturbed and does not participate in intramolecular processes. In principle, a spin-forbidden energy transfer assisted by the heavy Ir^{III} ion could take place from the Ir-^{1}A to the ^{3}Ir-A state, however, as noticed above, no sensitization of the Ir component luminescence was detected. The short lifetime of the Ir-^{1}A species could preclude such possibilities. Excitation of the Ir complex unit leads very rapidly to the ^{3}Ir-A excited state, from which energy transfer occurs to the triplet localized on the acceptor Ir-^{3}A with a $\Delta G^0 = -0.37$ eV. From the lifetimes of the model ^{3}Ir1, $\tau_0 = 740$ ns, and of the ^{3}Ir-A state, $\tau = 180$ ns, by making use of the relation $k = 1/\tau - 1/\tau_0$, a rate of 4.2×10^6 s^{-1} can be calculated for the energy-transfer process. The results at 77 K in a rigid matrix where the lifetime of the **Ir1** model, much longer than at room temperature ($\tau_0 = 80$ μs[13]) is more effectively quenched than at room temperature (see Figure S3 in the Supporting Information), are in perfect agreement with an energy-transfer-quenching mechanism. The rate of energy transfer is in fact little affected by the conditions of the medium.

Dyad D-Ir:[10] This dyad is made up of the D component, which can be easily oxidized ($E_{1/2} = 0.75$ V), and of the iridium complex that can be reduced at low potentials ($E_{1/2} = -0.75$ V) yielding a charge-separated state D^+-Ir^- with an energy of 1.5 eV. This is characterized by an extra electron localized on the metal complex, most probably on the ligand, and a hole on the donor. An electron-transfer process is thermodynamically possible upon excitation of either unit and in agreement, a quenching of the luminescent states localized on both units can be detected, Figures 2 and 3. The excited-state-quenching mechanism in the two cases will be different; 1) When the Ir complex is excited, a reductive quenching of its excited state will occur, that is, the electron will move from the HOMO localized on the donor to the HOMO localized on the Ir complex; 2) When the donor is excited, an electron will move from the LUMO localized on the donor to the LUMO on the Ir complex acceptor. The product will be the charge-separated state D^+-Ir^- in both cases. The reaction has a $\Delta G^0 = -0.93$ eV when

the initial state is ^{3}Ir-D and $\Delta G^0 = -1.43$ eV when the initial state is Ir-^{1}D, respectively. The high driving force for the latter reaction seems to be able to promote electron transfer also in glassy media at 77 K, whereas the former, characterized by a lower driving force is somehow slowed down by the rigidification of the solvent, as testified by the steady-state luminescence experiments at 77 K (see Figure S3 in the Supporting Information).

Transient-absorption spectroscopy shows that at the end of the picosecond pulse the only detectable product is the CS state D^+-Ir^-, indicating that the electron transfer has taken place within the experimental resolution of 20 ps and that excitation of both units leads to charge separation. This allows us to place a lower-limit rate of $5\times10^{10}\,s^{-1}$ for the charge-separation step that occurs with 100% yield. The D^+-Ir^- CS species decays back to the ground state with a lifetime of 70 ps, without leaving any absorbance ascribable to other intermediates.

Triad D-Ir-A: Similarly to the model dyad **D-Ir**, electron transfer from the excited states ^{1}D-Ir-A and D-^{3}Ir-A also occurs in the triad to yield the charge-separated state D^+-Ir^--A characterized by an energy level of 1.56 eV. However, in this case a further charge-separated state is present in the energy level diagram, corresponding to the FCS state D^+-Ir-A^-, with an energy of 1.26 eV. This is formed from the primary charge-separated state D^+-Ir^--A upon an electron-shift from the reduced Ir complex moiety ($E_{1/2} = -0.80$ V) to the nearby A unit ($E_{1/2} = -0.50$ V). The reaction is however not quantitative since it has to compete with the fast charge recombination of the D^+-Ir^--A species that occurs with a lifetime of 70 ps in the model dyad to form the ground state. In the triad the decay of the D^+-Ir^--A species is slightly faster, that is 60 ps. By making use of these lifetimes, a rate of $2.4\times10^9\,s^{-1}$ and a yield of approximately 14% can be calculated for the formation of the FCS state. The yield thus determined can be considered to be in reasonable agreement with the one directly determined with the benzophenone actinometer in the nanosecond flash photolysis experiments (see above), 7%; both determinations are in fact affected by large uncertainties and the yield can be averaged to a value of about 10%. The reason for this relatively low yield is due to the competition by the fast charge recombination to the ground state of the D^+-Ir^--A species. However the lifetime of the FCS state is remarkable; in air-purged and air-equilibrated solutions the intramolecular recombination lifetime was measured to be 120 μs and 100 μs, respectively. A low reaction rate of the FCS with O_2 of approximately $9\times10^5\,M^{-1}$ can be calculated.[29] It should now be recalled that excitation of the A component, absorbing approximately 45% of the photons at 355 nm, does not lead to any useful process but evolves into a triplet excited state D-Ir-^{3}A that leads to triad molecules with a single-radical site, either D^+-Ir-A or D-Ir-A^-, the intermolecular decay of which takes place in a bimolecular manner.

These results compare quite well with the most successful charge-separation systems based on tetrapyrroles or fullerene derivatives[1] and are among the best results achieved so far from different groups including our own, on metal-complex-based systems.[2,3] In particular, the modest sensitivity of the charge-separated-state lifetime to oxygen appears quite unique. The large 3.7-nm distance between the centers of the donor and acceptor units bearing the charges, and the very modest electronic coupling between the extremity components provided by benzamide linkers and by the interposition of the iridium metal complex have proven to be quite effective.

Conclusion

We have synthesized a triad based on an iridium(III) terpyridine-type core with an aromatic amine donor and a bisimide electron acceptor on opposite positions, the component models, and the simpler constituent dyad, and fully characterized them from an electrochemical, spectroscopic, and photophysical point of view. Upon excitation of the Ir and D moiety the dyad has proven to produce a fully charge-separated state, with the charges localized at the extremities of the rigid linear array, with a remarkably long lifetime. The presence of oxygen does not seem to alter the intramolecular recombination rate to a great extent, since we determined a lifetime of approximately 100 μs in air-equilibrated solutions and of approximately 120 μs in air-purged solutions. The complete disappearance of spectroscopic bands assigned to the cation and anion requires times of the order of milliseconds/seconds, and this slow process is identified as intermolecular recombination of triad molecules bearing either the reduced acceptor or the oxidized donors. This is one of the most successful examples of a charge-separation system based on a transition-metal complex if we consider the lifetime of the charge-separated state and the stability in the presence of air. The disadvantage of the system is the low yield of the formation of the fully charge-separated state, of the order of 10%. We are presently working on the modification of the structure of the triad to slow down the recombination of the initially formed CS state D^+-Ir^--A, with the aim of favoring the formation of the fully charge-separated state D^+-Ir-A^- with a better yield. A promising strategy seems to be the insertion of a further spacer between the Ir complex unit and the donor moiety.

Experimental Section

General methods: Oxygen- or moisture-sensitive reactions were performed by using Schlenk techniques in oven-dried glassware attached to a vacuum line. Dry solvents were distilled from suitable desiccants under argon. All other chemicals were purchased from commercial sources and were used without further purification. Column chromatography was carried out on silica gel 60 (Merck, 40–63 (fine) or 63–200 mesh). Thin layer chromatography (TLC) was performed on glass plates coated with silica gel 60 F_{254} (Merck). Elemental analyses were performed by the "Service de Microanalyse de l'Institut de Chimie" Strasbourg. ^{1}H NMR spectra were recorded with either Bruker WP200SY (200 MHz) or Bruker

AVANCE 400 (400 MHz) spectrometers with the deuterated solvent as the lock and residual solvent as the internal reference. The numbering schemes of the protons of the Ir complexes and the reference compounds are indicated in the Supporting Information (Figure S1). Electron spray ionization mass spectra (ESI MS) were recorded with a Bruker MicroTOF instrument. UV/Vis absorption spectra were recorded with a Kontron Instruments UVIKON 860 spectrometer at room temperature. Electrochemical experiments were performed with a three-electrode system consisting of a platinum working electrode, a platinum-wire counter electrode, and an SCE as reference electrode. The measurements were carried out under Ar gas, in degassed CH_3CN at 298 K using 0.1 M N-(nBu)$_4$PF$_6$ as the supporting electrolyte. An EG&G Princeton Applied Research Model 273A potentiostat connected to a computer was used for the cyclic voltammetry experiments.

The D^+ species was generated by the addition of one drop of Br_2 in the solution of compound **D** (6×10^{-5} M) in acetonitrile. The reduced acceptor A^- was generated in air-free acetonitrile by irradiating a solution of compound **A** (ca. 10^{-4} M) in the presence of [Ru(bpy)$_3$](PF$_6$)$_2$ (ca. 5×10^{-5} M) and triethanolamine: the excited state of the ruthenium complex transferred an electron to the acceptor and was reduced by the sacrificial donor triethanolamine.

For the photophysical experiments the solvents were spectrophotometric-grade acetonitrile at 295 K and butyronitrile at 77 K. Deaerated solutions were bubbled for 10 min with a stream of argon gas in home-modified 10 mm fluorescence cells. A Perkin–Elmer Lambda 5 UV/visible spectrophotometer and a Spex Fluorolog II spectrofluorimeter were used to acquire absorption and emission spectra. Emission quantum yields were determined after correction for the photomultiplier response, with reference to air-equilibrated Ir^{III}(3,5-ditertiobutylphenyl-2,2′;6′,2″-terpyridine)$_2$(PF$_6$)$_3$ with a $\Phi_{em}=0.022$ in air-saturated acetonitrile.[14] The photons absorbed by the unit of interest in the array (as calculated from the molar absorption coefficients) were used to determine the emission quantum yields (Φ_{em}). Luminescence lifetimes (τ) were obtained with an IBH single-photon-counting instrument upon excitation at 373 nm from a pulsed-diode source or with an apparatus based on a Nd:YAG laser (35 ps pulse duration, 355 nm, 0.5 mJ) and a Streak Camera with an overall resolution of 20 ps.[30] Transient-absorption spectra and lifetimes with picosecond resolution were determined by using a pump-probe apparatus with 30 ps resolution based on a Nd:YAG laser (355 nm, 3–4 mJ, 35 ps, 10 Hz).[30] Nanosecond laser flash photolysis experiments were performed by a system based on a Nd:YAG laser (JK Lasers, 355 nm, 1.5–8.5 mJ, 18 ns pulse) previously described by using a right-angle analysis on the excited sample.[31] The detection system could be operated either in "fast configuration" with a pulsed xenon lamp as the analyzing light and an overall resolution of about 15 ns, convenient for time ranges 15 ns–1 μs, or in a "slow configuration" with a steady xenon lamp and an overall resolution from 1 μs (depending on the load resistance), convenient for determinations in the range 2 μs–1 s. Relative yields of the various states were derived by comparing the absorbance of the species in the models ($\varphi=1$) with the absorbance of the species detected under the same experimental conditions as in the array, by taking into consideration only the fraction of photons absorbed by the moieties of interest within the array. We evaluated the absolute yield of the CS state by comparing the end-of-pulse A^- species absorbance against a benzophenone in air-free benzene actinometer. The parameters used were for the A^- species a molar absorption coefficient of 7000 M^{-1} cm^{-1} at 605 nm[24] and for the benzophenone triplet a molar absorption coefficient of 7220 M^{-1} cm^{-1} at 530 nm, and a $\Phi_T=1$.[32] Experimental uncertainties were estimated to be within 10% for lifetime determinations involving a simple exponential, 20% for lifetime determinations involving multiple exponentials or more complex kinetics, 15% for quantum yields, 20% for molar absorption coefficients, and 3 nm for emission and absorption peaks.

Syntheses: Compound **D** and complexes **Ir**, **Ir1**, **D-Ir** as well as the intermediate compounds **2**, **4**, and **5** were prepared according to literature procedures.[10,13]

***N*-(*p*-*t*Buphenyl)-naphthalene-1,8-dicarboxyanhydride-4,5-dicarboximide (1)**: 1,4,5,8-Naphthalenetetra-carboxydianhydride (707 mg, 2.64 mmol) was heated for 5 min at 120 °C in 5 mL DMF with EDC (200 mg, 1 mmol) under argon. *p*-*t*Bu-aniline (249 mg, 1.67 mmol) was added through the cooler. The solution was heated for 2 h at 120 °C. DMF was evaporated under vacuum and the crude was rapidly subjected to chromatography (SiO_2, CH_2Cl_2/MeOH 1%). The product **1** was obtained as a solid. Yield: 70% (490 mg). ^{1}H NMR ($CDCl_3$, 200 MHz): $\delta=8.88$ (s, 4H; H_A), 7.60 (d, 2H; H_{oA}, $^3J=8.4$ Hz), 7.26 (d, 2H; H_{mA}, $^3J=8.4$ Hz), 1.41 ppm (s, 9H; *t*Bu); elemental analysis calcd (%) for $C_{24}H_{17}NO_5$: C 72.17, H 4.29, N 3.51; found: C 72.32, H 4.38 N 3.32; MS (ES): m/z (calcd): 422.1 (422.09) $[M+Na]^+$.

***N*-(*p*-*t*Buphenyl)-*N*′-(*p*-benzoic acid)-naphthalene-1,8:4,5-tetracarboxydiimide (A)**: *p*-Amino benzoic acid (172 mg, 1.25 mmol) and compound **1** (467 mg, 1.17 mmol) were refluxed in 12.5 mL DMAc for 5 h. Water (10 mL) were added and the solution was placed in a fridge overnight. The precipitate was filtered and washed with hot MeOH and hot EtOAc. Compound **A** was obtained as a slightly brown solid. Yield: 80% (485 mg). ^{1}H NMR ([D$_6$]DMSO, 200 MHz): $\delta=8.74$ (s, 4H; H_A), 8.14 (d, $^3J=8.4$ Hz, 2H; H_a), 7.63 (d, $^3J=8.6$ Hz, 2H; H_{oA}), 7.60 (d, $^3J=8.6$ Hz, 2H; H_b), 7.39 (d, $^3J=8.4$ Hz, 2H; H_{mA}), 1.40 ppm (s, 9H; *t*Bu); elemental analysis calcd (%) for $C_{31}H_{22}N_2O_6$: C 71.81, H 4.28, N 5.40; found: C 72.02, H 4.38, N 5.32; MS (ES): m/z (calcd): 519.14 (519.15) $[M+H]^+$. The acid chloride derivative **3** was obtained by reaction of compound **A** with the oxalyl chloride in large excess and was used without further purification.

Ir(*t*Butpy)(tpy-PhNHC(O)-naphthalene-1,8:4,5-tetracarboxydiimide) (Ir-A): Compound **3** (crude prepared from 95 mg of compound **A**) was added slowly to a solution of compound **2** (65 mg, 0.047 mmol) in DMAc (2 mL) and pyridine (0.5 mL). The resulting solution was stirred for 2 h. After precipitation with water/KPF_6, the crude was separated by chromatography on silica with acetonitrile/H_2O/KNO_3 from 100:0:0 to 100:5:0.5 as eluent. After anion exchange, dyad **Ir-A** was obtained as a yellow solid with 46% yield (41 mg). ^{1}H NMR (CD_3CN, 400 MHz): $\delta=9.29$ (s, 1H; NH), 9.11 (s, 2H; $A_{3'}A_{5'}$), 9.04 (s, 2H; $H_3H_{5'}$), 8.80–8.74 (m, 4H; H_3), 8.67 (s, 4H; H_A), 8.30–8.20 (m, 10H; $H_4H_{o1}H_{o2}H_{m2}$), 7.99 (d, $^4J=1.7$ Hz, 2H; H_o), 7.87 (t, $^4J=1.7$ Hz, 1H; H_p), 7.75–7.71 (ddd, $^3J=10.2$ Hz, $^4J=5.7$ Hz, $^5J=0.9$ Hz, 4H; H_6), 7.64 (d, $^3J=8.5$ Hz, 2H; H_{oA}), 7.62 (d, $^3J=8.4$ Hz, 2H; H_{m1}), 7.54–7.49 (m, 4H; H_5), 7.33 (d, 2H; H_{ma}), 1.53 (s, 18H; *t*Bu), 1.40 ppm (s, 9H; *t*Bu′); MS (MALDI-TOF): m/z (calcd): 1438 (1438) $[M-3PF_6]^+$, 1583 (1583) $[M-2PF_6]^+$, 1727 (1728) $[M-PF_6]^+$; UV/Vis (CH_3CN): 253 (68900), 280 (69200), 340 (40700), 358 (49600), 379 nm (58000 M^{-1} cm^{-1}).

Tpy-C$_6$H$_4$-NHC(O)-C$_6$H$_4$-N(C$_6$H$_4$OMe)$_2$ (6): DMAP (353 mg, 2.73 mmol, 3.2 equiv) and EDC (281 mg, 1.47 mmol, 1.7 equiv) were added to a solution of compound **4** (450 mg, 1.28 mmol, 1.5 equiv) in distilled CH_2Cl_2 (4 mL). After few minutes stirring, the solution became yellow. Tpy-C_6H_4-NH_2 (**5**) (275 mg, 0.85 mmol, 1 equiv) was added and the solution was protected from light and stirred under argon for 24 h. Then DMF (1.5 mL) was added and the CH_2Cl_2 was removed under reduced pressure. Water (5 mL) and saturated $NaHCO_3$ solution (5 mL) were added resulting in a bright yellow precipitate which was filtered off and washed with water. Alumina chromatography with CH_2Cl_2 afforded compound **6** as a bright yellow solid. Yield: 92% (514 mg, 0.78 mmol). ^{1}H NMR ([D$_6$]DMSO, 300 MHz): $\delta=10.15$ (s, 1H; NH), 8.74 (dt, $^3J=4.7$ Hz, $^4J=0.8$ Hz, 2H; H_6), 8.70 (s, 2H; $H_{3'5'}$), 8.65 (d, $^3J=8$ Hz, 2H; H_3), 8.04–7.89 (m, 6H; $H_4H_{o3}H_{m3}$), 7.81 (d, $^3J=8.9$ Hz, 2H; H_{o4}), 7.50 (ddd, $^3J=7.4$ Hz, $^3J=5.8$ Hz, $^4J=0.9$ Hz, 2H; H_5), 7.10 (d, $^3J=9.0$ Hz, 4H; H_a), 6.94 (d, $^3J=9.0$ Hz, 4H; H_b), 6.73 (d, $^3J=8.9$ Hz, 2H; H_{m4}), 3.72 ppm (s, 6H; CH_3); ^{13}C NMR ([D$_6$]DMSO, 75 MHz): $\delta=165.5$, 156.9, 156.4, 156.0, 152.1, 149.6, 149.2, 139.6, 139.5, 137.0, 133.8, 128.4, 128.0, 127.7, 124.7, 123.9, 121.5, 120.3, 118.5, 117.8, 115.0, 55.6 ppm; elemental analysis calcd (%) for $C_{42}H_{33}N_5O_3$: C 76.96, H 5.07, N 10.68; found: C 76.74, H 5.15, N 10.32; MS (ES): m/z (calcd): 656.26 (656.26) $[M+H]^+$.

[Ir{tpy-C$_6$H$_4$-NHC(O)-C$_6$H$_4$-N(C$_6$H$_4$OMe)$_2$}]Cl$_3$ (7): Compound **6** (442 mg, 0.67 mmol) was dissolved at reflux in a mixture of EtOH (50 mL) and THF (2 mL). A solution of $IrCl_3$ (201 mg, 0.67 mmol) in EtOH (50 mL) was added dropwise over 15 min. The suspension was refluxed for 4 h protected against light. The mixture was evaporated to dryness and dissolved in DMSO/CH_2Cl_2. Fe^{2+} salts were added and the crude was separated by chromatography on an alumina column eluted

with CH_2Cl_2/MeOH from 0 to 8%. Compound **7** was obtained as an orange-red solid in 30% yield (191 mg, 0.20 mmol). ^{1}H NMR ([D$_6$]DMSO, 300 MHz): $\delta = 10.25$ (s, 1H; NH), 9.20 (d, $^3J = 5.1$ Hz, 2H; H_6), 9.07 (s, 2H; $H_{3'5'}$), 8.89 (d, $^3J = 7.6$ Hz, 2H; H_3), 8.28 (dd, $^3J = 7.6$ Hz, $^3J = 6.9$ Hz, 2H; H_4), 8.22 (d, $^3J = 8.4$ Hz, 2H; H_{o3}), 8.06 (d, $^3J = 8.5$ Hz, 2H; H_{m3}), 7.95 (t, $^3J = 6.9$ Hz, 2H; H_5), 7.82 (d, $^3J = 8.7$ Hz, 2H; H_{o4}), 7.13 (d, $^3J = 8.8$ Hz, 4H; H_a), 6.97 (d, $^3J = 8.8$ Hz, 4H; H_b), 6.74 (d, $^3J = 8.8$ Hz, 2H; H_{m4}), 3.73 (s, 6H; CH_3); MS (ES): *m*/*z* (calcd): 976.11 (976.12) $[M+Na]^+$, 918.16 (918.15) $[M-Cl]^+$.

[Ir(tpy-C$_6$H$_4$-NHC(O)-C$_6$H$_4$-N(C$_6$H$_4$OMe)$_2$)(tpy-C$_6$H$_4$-NH$_2$)](PF$_6$)$_3$ (8): A mixture of compound **7** (94 mg, 0.098 mmol) and tpy- **C$_6$H$_4$**-NH_2 (**5**) (32 mg, 0.099 mmol) in ethylene glycol (30 mL) was sonicated for 20 min. It was degassed by using three vacuum/argon cycles and was heated from room temperature to 160 °C under argon, at which temperature it remained for 20 min. The solution was allowed to cool to room temperature and water and a saturated solution of KPF_6 were added. The precipitate was filtered off and taken up with acetonitrile. Chromatography on a silica column (eluted with MeCN/water/KNO_3 from 100:0:0 to 100:10:1) gave an almost pure fraction of the desired product. This fraction was purified on TLC plates (SiO_2, 20×20 cm, 0.5 mm) and was eluted with 100:18:1.8 MeCN/water/KNO_3. Compound **8** was obtained as a bright red solid in 42% yield (67 mg, 0.042 mmol). ^{1}H NMR (CD_3CN, 400 MHz): $\delta = 9.08$ (s, 2H; $D_{3'5'}$), 8.98 (s, 1H; NH), 8.96 (s, 2H; $H_{3'5'}$), 8.72 (td, $^3J = 8.6$ Hz, $^4J = 0.6$ Hz, 2H; H_3D_3), 8.27–8.20 (m, 6H; $H_4D_4H_{o3}$), 8.16 (d, $^3J = 8.9$ Hz, 2H; H_{m3}), 8.08 (d, $^3J = 8.8$ Hz, 2H; H_{o1}), 7.84 (d, $^3J = 8.9$ Hz, 2H; H_{o4}), 7.74–7.69 (2dd, $^3J = 11.7$ Hz, $^4J = 0.8$ Hz, 4H; H_6D_6,), 7.53–7.46 (m, 4H; H_5D_5), 7.21 (d, $^3J = 9$ Hz, 4H; H_a), 6.99 (d, $^3J = 9.0$ Hz, 4H; H_b), 6.89 (d, $^3J = 9.0$ Hz, 2H; H_{m1}), 6.84 (d, $^3J = 8.8$ Hz, 2H; H_{m4}), 5.10 (s, 2H; NH_2), 3.81 ppm (s, 6H; CH_3); MS (ES): *m*/*z* (calcd): 390.8 (390.7) $[M-3PF_6]^{3+}$, 658.8 (658.5) $[M-2PF_6]^{2+}$.

Triad D-Ir-A: Compound **D-Ir-A** (30 mg, 0.018 mmol) dissolved in DMAc (2.5 mL) was added to a suspension of compound **3** (prepared from 50 mg, 0.098 mmol of compound **A**) in DAMc (1 mL) and a few drops of pyridine. The mixture was stirred for 4 h at room temperature under argon. H_2O and a saturated solution of KPF_6 in water were added. The precipitate was filtered off and taken up with acetonitrile. The crude was purified on a silica column eluted with MeCN/H_2O/KNO_3 from 100:0:0 to 100:9:0.9. Triad **D-Ir-A** was obtained as an orange-yellow solid with 45% yield (18 mg, 0.008 mmol). ^{1}H NMR (CD_3CN, 400 MHz): $\delta =$ 9.37 (s, 1H; NH_A), 9.14 (s, 2H; $H_{3'5'}$), 9.11 (s, 2H; $D_{3'5'}$), 9.01 (s, 1H; NH_D), 8.82–8.74 (m, 4H; H_3D_3), 8.78 (d, $^3J = 1.7$ Hz, 4H; H_A), 8.30 (d, $^3J = 9.0$ Hz, 2H; H_{o1}), 8.28–8.22 (m, 10H; $H_4D_4H_{o3}H_{m1}H_{o2}$), 8.16 (d, $^3J =$ 8.8 Hz, 2H; H_{m3}), 7.8 (d, $^3J = 9.0$ Hz, 2H; H_{o4}), 7.75–7.73 (m, 4H; H_6D_6), 7.66 (d, $^3J = 8.8$ Hz, 2H; H_{mA}), 7.64 (d, $^3J = 8.7$ Hz, 2H; H_{m2}), 7.53–7.49 (m, 4H; H_5D_5), 7.34 (d, $^3J = 8.7$ Hz 2H; H_{oA}), 7.19 (d, $^3J = 9.0$ Hz, 4H; H_a), 6.99 (d, $^3J = 9.0$ Hz, 4H; H_b), 6.83 (d, $^3J = 8.9$ Hz, 2H; H_{m4}), 3.82 (s, 6H; CH_3), 1.42 ppm (s, 9H; *t*Bu); MS (ES): *m*/*z* (calcd): 1673.7 (1673) $[MH-3PF_6]^+$.

Acknowledgements

We thank CNR of Italy (PM-P04-ISTM-C1/ISOF-M5), CNRS (France), the Ministero dell'Istruzione, dell'Universita' e della Ricerca of Italy (FIRB, RBNE019H9K) and COST D31 for financial support. E.B. acknowledges support from the French Ministry of Education. We thank also Johnson Matthey Inc. for a loan of $IrCl_3$.

[1] a) D. Gust, T. A. Moore, A. L. Moore, A. N. MacPherson, A. Lopez, J. M. DeGraziano, I. Gouni, E. Bittersman, G. R. Seely, F. Gao, R. A. Nieman, X. C. Ma, L. J. Demanche, S.-C. Hung, D. K. Luttrull, S.-J. Lee, P. K. Kerrigan, *J. Am. Chem. Soc.* **1993**, *115*, 11141–11152; b) K. A. Joliffe, T. D. Bell, K. P. Ghiggino, S. J. Langford, M. N. Paddon Row, *Angew. Chem.* **1998**, *110*, 960–963; *Ang. Chem. Int. Ed. Engl.* **1998**, *37*, 916–919; c) H. Imahori, D. M. Guldi, K. Tamaki, Y. Yoshida, C. Luo, Y. Sakata, S. Fukuzumi, *J. Am. Chem. Soc.* **2001**, *123*, 6617–6628; d) H. Imahori, Y. Sekiguchi, Y. Kashiwagi, T. Sato, Y. Araki, O. Ito, H. Yamada, S. Fukuzumi, *Chem. Eur. J.* **2004**, *10*, 3184–3196.

[2] a) T. J. Meyer, *Acc. Chem. Res.* **1989**, *22*, 163–170; b) J. H. Alstrum-Acevedo, M. K. Brennaman, T. J. Mayer, *Inorg. Chem.* **2005**, *44*, 6802–6827; c) L. De Cola, V. Balzani, F. Barigelletti, L. Flamigni, P. Belser, A. von Zelewsky, M. Frank, F. Vogtle, *Inorg. Chem.* **1993**, *32*, 5228–5238; d) I. M. Dixon, J.-P. Collin, J.-P. Sauvage, L. Flamigni, *Inorg. Chem.* **2001**, *40*, 5507–5517; e) C. Chiorboli, S. Fracasso, F. Scandola, S. Campagna, S. Serroni, R. Konduri, F. M. MacDonnell, *Chem. Commun.* **2003**, *14*, 1658–1659; f) S. Chakraborty, T. J. Wadas, H. Hester, R. Schmehl, R. Eisenberg, *Inorg. Chem.* **2005**, *44*, 6865–6878.

[3] M. Borgström, N. Shaikh, O. Johansson, M. F. Anderlund, S. Styring, B. Åkermark, A. Magnuson, L. Hammarström, *J. Am. Chem. Soc.* **2005**, *127*, 17504–17515.

[4] a) K. Ohkubo, H. Kotani, J. Shao, Z. Ou, K. M. Kadish, G. Li, R. K. Pandey, M. Fujitsuka, O. Ito, H. Imahori, S. Fukuzumi, *Angew. Chem.* **2004**, *116*, 871–874; *Angew. Chem. Int. Ed.* **2004**, *43*, 853–856; b) S. Fukuzumi, H. Kotani, K. Ohkubo, S. Ogo, N. Tkachenko, H. Lemmetyinen, *J. Am. Chem. Soc.* **2004**, *126*, 1600–1601.

[5] a) A. C. Benniston, A. Harriman, P. Y. Li, J. P. Rostron, J. W. Verhoeven, *Chem. Commun.* **2005**, 4520–4522; b) Ohkubo, H. Kotani, S. Fukuzumi, *Chem. Commun.* **2005**, 4520–4522; c) A. C. Benniston, A. Harriman, P. Li, J. P. Rostron, H. J. van Ramesdonk, M. M. Groeneveld, H. Zhang, J. W. Verhoeven, *J. Am. Chem. Soc.* **2005**, *127*, 16054–16064; d) J. W. Verhoeven, H. J. van Ramesdonk, M. M. Groeneveld, A. C. Benniston, A. Harriman, *ChemPhysChem* **2005**, *6*, 2551–2560.

[6] E. Baranoff, J.-P. Collin, L. Flamigni, J.-P. Sauvage, *Chem. Soc. Rev.* **2004**, *33*, 147–155, and references therein.

[7] I. M. Dixon, J.-P. Collin, J.-P. Sauvage, L. Flamigni, S. Encinas, F. Barigelletti, *Chem. Soc. Rev.* **2000**, *29*, 385–391.

[8] See, for example: a) G. P. Wiederrecht, M. P. Niemczyk, W. A. Svec, M. R. Wasielewski, *J. Am. Chem. Soc.* **1996**, *118*, 81–88; b) T. Yamazaki, I. Yamazaki, A. Osuka, *J. Phys. Chem. B* **1998**, *102*, 7858–7865; c) L. Flamigni, M. R. Johnston, L. Giribabu, *Chem. Eur. J.* **2002**, *8*, 3938–3947; d) O. Johansson, M. Borgström, R. Lomoth, M. Palmblad, J. Bergquist, L. Hammarström, L. Sun, B. Åkermark, *Inorg. Chem.* **2003**, *42*, 2908–2918.

[9] See, for example: a) T. D. M. Bell, A. Stefan, S. Masuo, T. Vosch, M. Lor, M. Cotlet, J. Hofkens, S. Bernhardt, K. Müllen, M. van der Auweraer, J. W. Verhoeven, F. C. De Schryver, *ChemPhysChem* **2005**, *6*, 942–948; b) A. D. Sandanayaka, H. Sasabe, Y. Araki, Y. Furusho, O. Ito, T. Takata, *J. Phys. Chem. A* **2004**, *108*, 5145–5155.

[10] E. Baranoff, I. M. Dixon, J.-P. Collin, J.-P. Sauvage, B. Ventura, L. Flamigni, *Inorg. Chem.* **2004**, *43*, 3057–3066.

[11] J. C. Sheehan, P. A. Cruickshank, G. L. Broshart, *J. Org. Chem.* **1961**, *26*, 2525–2528.

[12] A view of the crystal structure of compound **6** is given in the Supporting Information (see Figure S2).

[13] L. Flamigni, B. Ventura, F. Barigelletti, E. Baranoff, J.-P. Collin, J.-P. Sauvage, *Eur. J. Inorg. Chem.* **2005**, 1312–1318.

[14] J. P. Collin, I. M. Dixon, J.-P. Sauvage, J. A. G. Williams, F. Barigelletti, L. Flamigni, *J. Am. Chem. Soc.* **1999**, *121*, 5009–5016.

[15] W. Leslie, R. A. Poole, P. R. Murray, L. J. Yellowlees, A. Beeby, J. A. G. Williams, *Polyhedron* **2004**, *23*, 2769–2777.

[16] W. Leslie, A. S. Bastanov, J. A. K. Howard, J. A. G. Williams, *Dalton Trans.* **2004**, 623–631.

[17] For the excitation at 320 nm, the relative absorbance derived from the molar absorption coefficients of the models are for **Ir-D**: 40% on **D**, 60% on **Ir**; for **D-Ir-A**: 30% on **D**, 60% on **Ir**, 10% on **A**. For the excitation at 357 nm the data are for **Ir-A**: 50% on **A**, 50% on **Ir**, for **D-Ir-A**: 40% on **A**, 45% on **Ir**, 15% on **D**.

[18] T. C. Barros, S. Brochsztain, V. G. Toscano, P. B. Filho, M. J. Politi, *J. Photochem. Photobiol. A* **1997**, *111*, 97–104.

[19] G. P. Wiederrecht, M. P. Niemczyk, W. A. Svec, M. A. Wasielewski, *J. Am. Chem. Soc.* **1996**, *118*, 81–88.

[20] S. E. Miller, A. S. Lukas, E. Marsh, P. Bushard, M. R. Wasielewski, *J. Am. Chem. Soc.* **2000**, *122*, 7802–7810.
[21] It should in fact be noticed that the build-up of the spectrum is slow compared to the excitation profile reported in Figure 5 and this could support the assignment of the band as due to the excimeric singlet state ^{1}AA.
[22] B. M. Aveline, S. Matsugo, R. W. Redmond, *J. Am. Chem. Soc.* **1997**, *119*, 11785–11795.
[23] A very small increase in lifetime in the decay of approximately 135 ps is detected at 760 nm and assigned to the absorption of an excited species formed by a biphotonic process, that is, to $A^{-}*$.[24] In agreement, its contribution increases with the photon flux.
[24] D. Gosztola, M. P. Niemczyk, W. A. Svec, A. S. Lucas, M. R. Wasielewski, *J. Phys. Chem. A* **2000**, *104*, 6545–6551.
[25] F. Wilkinson, W. P. Helman, A. B. Ross, *J. Phys. Chem. Ref. Data* **1995**, *24*, 663–1021.
[26] A. P. Darmanyan, W. S. Jenks, P. Jardon, *J. Phys. Chem. A* **1998**, *102*, 7420–7426.
[27] C. Schweitzer, R. Schmidt, *Chem. Rev.* **2003**, *103*, 1685–1757.
[28] At high concentration of triad **D-Ir-A**, the reaction D-Ir-^{3}A + D-Ir-A $\rightarrow$ D^+-Ir-A + D-Ir-A^- prevails and occurs essentially by the bimolecular recombination D^+-Ir-A + D-Ir-A^- $\rightarrow$ D-Ir-A.
[29] The solubility of O_2 in air-saturated acetonitrile is 1.9×10^{-3} from S. L. Murov, I. Carmichael, G. L. Hugh, *Handbook of Photochemistry*, Marcel Dekker, New York, **1993**, p. 289.
[30] L. Flamigni, A. M. Talarico, S. Serroni, F. Puntoriero, M. J. Gunter, M. R. Johnston, T. J. Jeynes, *Chem. Eur. J.* **2003**, *9*, 2649–2659, and references therein.
[31] L. Flamigni, *J. Chem. Soc. Faraday Trans. 1* **1994**, *90*, 2331–2336.
[32] I. Carmichael, G. L. Hug, *J. Phys. Chem. Ref. Data* **1986**, *15*, 1–250.

Received: January 3, 2006
Published online: June 29, 2006

